Journal of Experimental Botany, Vol. 61, No. 4, pp. 1041–1051, 2010
doi:10.1093/jxb/erp374 Advance Access publication 21 December, 2009
This paper is available online free of all access charges (see http://jxb.oxfordjournals.org/open_access.html for further details)

Journal of Experimental Botany
www.jxb.oxfordjournals.org

RESEARCH PAPER

Metabolic turnover analysis by a combination of *in vivo* ^{13}C-labelling from $^{13}CO_2$ and metabolic profiling with CE-MS/MS reveals rate-limiting steps of the C_3 photosynthetic pathway in *Nicotiana tabacum* leaves

Tomohisa Hasunuma[1,†], Kazuo Harada[2], Shin-Ichi Miyazawa[1], Akihiko Kondo[3], Eiichiro Fukusaki[2] and Chikahiro Miyake[1,*]

[1] Research Institute of Innovative Technology for the Earth (RITE), 9-2 Kizugawadai, Kizugawa-shi, Kyoto 619-0292 Japan
[2] Department of Biotechnology, Graduate School of Engineering, Osaka University, 2-1 Yamadaoka, Suita, Osaka 565-0871, Japan
[3] Department of Chemical Science and Engineering, Graduate School of Engineering, Kobe University, 1-1 Rokkodai, Nada, Kobe 657-8501, Japan

[†] Present address: Organization of Advanced Science and Technology, Kobe University, 1-1 Rokkodai, Nada, Kobe, 657-8501, Japan.
* Present address and to whom correspondence should be sent: Department of Biological and Environmental Science, Faculty of Agriculture, Kobe University, 1-1 Rokkodai, Nada, Kobe 657-8501, Japan. E-mail: cmiyake@hawk.kobe-u.ac.jp

Received 7 September 2009; Revised 22 November 2009; Accepted 24 November 2009

Abstract

Understanding of the control of metabolic pathways in plants requires direct measurement of the metabolic turnover rate. Sugar phosphate metabolism, including the Calvin cycle, is the primary pathway in C_3 photosynthesis, the dynamic status of which has not been assessed quantitatively in the leaves of higher plants. Since the flux of photosynthetic carbon metabolism is affected by the CO_2 fixation rate in leaves, a novel *in vivo* ^{13}C-labelling system was developed with $^{13}CO_2$ for the kinetic determination of metabolic turnover that was the time-course of the ^{13}C-labelling ratio in each metabolite. The system is equipped with a gas-exchange chamber that enables real-time monitoring of the CO_2 fixation rate and a freeze-clamp that excises a labelled leaf concurrently with quenching the metabolic reactions by liquid nitrogen within the photosynthesis chamber. Kinetic measurements were performed by detecting mass isotopomer abundance with capillary electrophoresis-tandem mass spectrometry. The multiple reaction monitoring method was optimized for the determination of each compound for sensitive detection because the amount of some sugar phosphates in plant cells is extremely small. Our analytical system enabled the *in vivo* turnover of sugar phosphates to be monitored in fresh tobacco (*Nicotiana tabacum*) leaves, which revealed that the turnover rate of glucose-1-phosphate (G1P) was significantly lower than that of other sugar phosphates, including glucose-6-phosphate (G6P). The pool size of G1P is 12 times lower than that of G6P. These results indicate that the conversion of G6P to G1P is one of the rate-limiting steps in the sugar phosphate pathway.

Key words: Capillary electrophoresis-tandem mass spectrometry (CE-MS/MS), $^{13}CO_2$, *in vivo* labelling, metabolic turnover, photosynthesis, sugar phosphate.

Introduction

To determine the limiting steps of photosynthesis and factors that influence carbon allocation, studies of photosynthetic CO_2 assimilation in plant leaves have focused on the regulation of carbohydrate metabolism. In higher plants, starch and sucrose, which are the major products of photosynthetic carbon metabolism, are biosynthesized from CO_2 via sugar phosphates and sugar nucleotides (Fig. 1). The biosynthetic pathway is regulated by metabolic reactions involving sugar nucleotides (Dennis and Blakeley, 2000; Zeeman *et al.*, 2007); that is, ADP-glucose

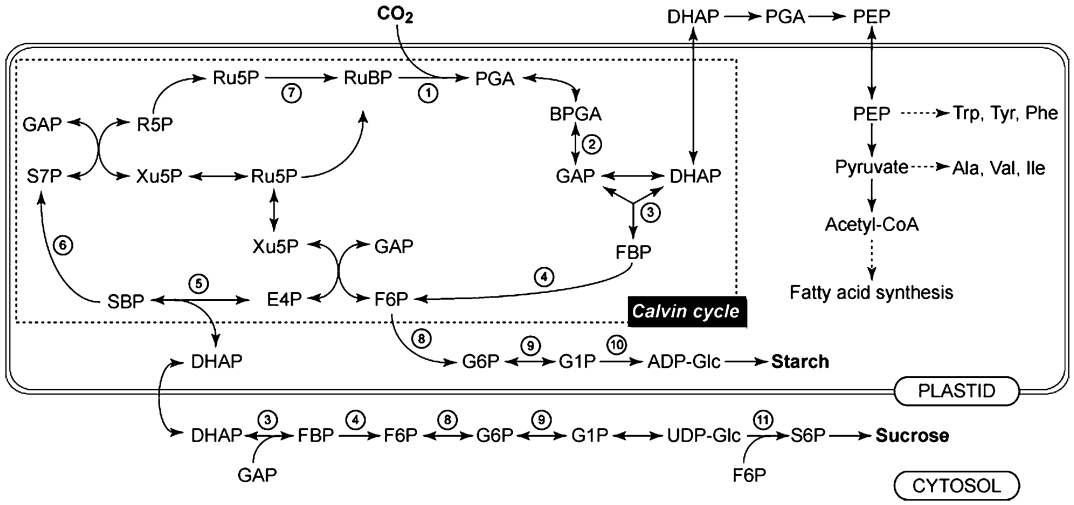

Fig. 1. The path of carbon in photosynthesis in a tobacco leaf. Abbreviations: ADP-Glc, adenosine-5′-diphosphate glucose; BPGA, 1,3-*bis*phosphoglycerate; DHAP, dihydroxyacetonephosphate; E4P, erythrose-4-phosphate; FBP, fructose-1,6-*bis*phosphate; F6P, fructose-6-phosphate; GAP, glyceraldehyde-3-phosphate; G1P, glucose-1-phosphate; G6P, glucose-6-phosphate; PEP, phosphoenolpyruvate; PGA, 3-phosphoglycerate; R5P, ribose-5-phosphate; RuBP, ribulose-1,5-*bis*phosphate; Ru5P, ribulose-5-phosphate; S6P, sucrose-6-phosphate; S7P, sedoheptulose-7-phosphate; SBP, sedoheptulose-1,7-*bis*phosphate; UDP-Glc, uridine-5′-diphosphate glucose; Xu5P, xylulose-5-phosphate. Numbers in circles denote enzymes as follows: (1) RuBP carboxylase/oxygenase (Rubisco); (2) GAP dehydrogenase; (3) FBP aldolase; (4) fructose-1,6-*bis*phosphatase (FBPase); (5) SBP aldolase; (6) sedoheptulose-1,7-*bis*phosphatase (SBPase); (7) phosphoribulokinase; (8) phosphoglucose isomerase (PGI); (9) phosphoglucomutase (PGM); (10) ADP-glucose pyrophosphorylase; (11) sucrose phosphate synthase.

pyrophosphorylase, which converts glucose-1-phosphate (G1P) into ADP-glucose, regulates starch content, and sucrose phosphate synthase, which converts UDP-glucose into sucrose-6-phosphate, regulates sucrose content. However, much controversy exists over the rate-limiting step of the metabolic pathway from CO_2 to G1P (Fig. 1).

Mathematical modelling of the metabolic pathway has suggested the possibility that several enzymes, ribulose-1,5-*bis*phosphate carboxylase/oxygenase (Rubisco), sedoheptulose-1,7-*bis*phosphatase (SBPase), and fructose 1,6-*bis*phosphate aldolase, control the flux of C_3 photosynthetic carbon metabolism (Giersch, 2000; Poolman *et al.*, 2000; Zhu *et al.*, 2007). On the other hand, modifications of the activities of these enzymes through genetic engineering have demonstrated the presence of other regulatory steps of carbon flow in plants (reviewed in Tamoi *et al.*, 2005). For example, in antisense plants for plastidial fructose-1,6-*bis*phosphatase (FBPase) and SBPase, the rate of photosynthesis was significantly diminished in proportion to the decrease in the respective enzyme activity due to a decrease in the ribulose-1,5-*bis*phosphate (RuBP) regeneration capacity in the Calvin cycle (Koßmann *et al.*, 1994; Harrison *et al.*, 1998, 2001; Ölçer *et al.*, 2001). This suggests that the photosynthetic carbon flow is more sensitive to a decrease in FBPase and SBPase activity. Also, by using a decreased-activity mutant of phosphoglucose isomerase (PGI) that catalyses the reversible conversion of fructose-6-phosphate (F6P) to glucose-6-phosphate (G6P) in the cytosol and chloroplasts, Kruckeberg *et al.* (1989) showed that the chloroplast isoenzyme exerted control over the rate of starch synthesis in saturating light intensity and CO_2, but not at low light intensity. By contrast, in transgenic plants with reduced levels of glyceraldehyde-3-phosphate dehydrogenase, phosphoribulokinase and aldolase had little effect on photosynthesis (Paul *et al.*, 1995; Price *et al.*, 1995; Haake *et al.*, 1998). These data indicate that these enzymes are present at levels well in excess of that required to sustain a continued rate of CO_2 assimilation. Thus, estimates based on metabolic simulation have not necessarily been the same as the results of metabolic engineering. In mathematical modelling, enzyme kinetics is used as one of the parameters which is determined *in vitro* and does not always reflect the turnover of *in vivo* metabolites. On the other hand, the result of changes in the accumulation levels of major products such as hexose, sucrose, and starch in transgenic plants are also not enough to account for the dynamic metabolic flux.

When metabolism is in a dynamic steady-state, *in vivo* metabolites are replaced with newly synthesized compounds at a constant rate and the total amount remains unchanged. In order to discuss metabolic flux and the rate-limiting step in the pathway, direct measurement of metabolic turnover is required (defined as the change of the newly incorporated carbon to total carbon ratio in a metabolite with respect to time). Thus, the aim was to develop a system to analyse *in vivo* turnover of metabolic intermediates involved in the sugar phosphate pathway and in sucrose and starch synthesis quantitatively in higher plants.

So far, the labelling of metabolites using stable isotope tracing has been used for the determination of *in vivo* metabolic turnover by detection with mass spectrometry (MS) or nuclear magnetic resonance (NMR) (reviewed in

Schwender, 2008). Since MS detects ionized compounds separated by their mass to charge ratio (*m*/*z*), the *m*/*z* of ^{13}C-labelled compounds is increased by an amount equal to the number of stable isotopes incorporated. Therefore, by determining the ratio of intensity of the monoisotopic ion and its isotopic ions, the ratio of stable isotope labelling can be quantified. As experimental materials for the labelling, tissue cultures such as tomato suspension cells, developing seeds of rapeseed, *Catharanthus roseus* hairy root, and potato tuber have the advantages that metabolites can be labelled from ^{13}C-sugar under strictly controlled culture conditions (Schwender, 2008). However, for the analysis of biosynthetic pathways of the photosynthetic products, it is necessary to feed labelled CO_2 as a sole carbon source.

In the case of labelling photosynthetic tissues such as leaves in higher plants, highly standardized photosynthesis conditions should be required for accurate kinetic measurements. Recently, Huege *et al.* (2007) labelled whole plants such as *Arabidopsis thaliana* and *Oryza sativa* with $^{13}CO_2$ as the carbon source in an atmospherically controlled, air-tight growth chamber where the average ^{13}C-enrichment ±standard deviation (SD) was 91.5±10.5% for shoots and 90.2±9.7% for roots of *A. thaliana*. Subsequently, the authors performed dynamic isotope dilution by unlabelled CO_2 to determine the ^{13}C half-life of soluble metabolites such as organic acids, amino acids, and sucrose using GC-MS. The authors succeeded in determining the metabolite and organ-specific ^{13}C-half-life. Nevertheless, variability among experiments was observed for some compounds, which may have resulted from slight environmental changes.

Since the flux through the photosynthetic metabolic pathway is influenced by photosynthetic rate (Farquhar *et al.*, 1980), factors affecting photosynthesis should be strictly controlled in ^{13}C-labelling for accurate measurement of *in vivo* turnover. In the present study, *in vivo* labelling of tobacco (*Nicotiana tabacum*) leaves by $^{13}CO_2$ was carried out in a gas-exchange chamber that enabled real-time monitoring of the CO_2 assimilation rate. Thus, the photosynthetic environmental conditions such as light intensity, CO_2 concentration, relative humidity, and temperature were controlled in the chamber. The experiment under different CO_2 concentration would reveal the influence of photosynthesis rate on the turnover rate of intermediates in the photosynthetic metabolic pathway. Also, since metabolic intermediates involved in photosynthesis turn over extremely fast (Sharkey *et al.*, 1986), the labelling time must be accurate. Thus, a freeze-clamp was used that excised a labelled segment concurrently with quenching the metabolic reaction by liquid nitrogen in the photosynthesis chamber.

Metabolic intermediates such as sugar phosphates and sugar nucleotides are highly polar molecules and are present as minor components in plant cells, which require efficient separation and a sensitive detection system for qualitative and quantitative analysis. Thus, an analytical system was developed that determines the ^{13}C-labelling rate of these compounds in plant leaves by using capillary electrophoresis-tandem mass spectrometry (CE-MS/MS) with multiple reaction monitoring (MRM) detection.

In the present study, a novel system was developed for dynamic metabolic analysis of the C_3 photosynthetic pathway in leaves by the combination of *in vivo* ^{13}C-labelling from $^{13}CO_2$ and metabolic profiling with CE-MS/MS. The system enabled monitoring of the *in vivo* turnover of sugar phosphates, which revealed that the turnover rate of G1P was significantly lower than that of other sugar phosphates including G6P. This result indicates that the conversion of G6P into G1P would be a rate-limiting step in sugar phosphate metabolism.

Materials and methods

Plant growth conditions

Wild-type tobacco plants (*Nicotiana tabacum* L. cv. Xanthi) were grown at 16/8 h day/night cycles at 25 °C and 50–60% relative humidity. Photon flux density was 300 μmol photons m^{-2} s^{-1}. Seedlings were kept in pots (0.7 dm^3 $plant^{-1}$) containing Metro-Mix350 (Sun Gro Horticulture, British Columbia, Canada), and were watered daily. Plants were fertilized with 500-fold diluted Hyponex solution (Hyponex Japan, Osaka) three times a week. Tobacco plants at 6–8 weeks old were used for $^{13}CO_2$-feeding experiments.

$^{13}CO_2$-feeding experiment

One fully expanded leaf was clamped in a 0.067 dm^3 aluminium gas-exchange chamber equipped with a freeze-clamp (Kohshin Rigakaku Seisakusho, Tokyo, Japan) that had a glass window to admit light. A photon flux of 1000 μmol m^{-2} s^{-1} was provided by a PCX-UHX-150 light source (Nippon PI, Tokyo, Japan). The CO_2 concentration of the air containing a 20% O_2 stream was regulated using a gas blender (Ollie, Osaka, Japan) to mix nitrogen, CO_2 (either $^{12}CO_2$ or $^{13}CO_2$) and oxygen from gas cylinders. The mixture of gases was saturated with water vapour at 16 °C using an LI-610 portable dew point generator (Li-Cor, Lincoln, NE, USA). The chamber temperature was controlled at 25 °C by a flow of water from an EL-15 refrigerated water bath (TAITEC, Saitama, Japan). The chamber contained sensors for chamber air and leaf temperature with a thermocouple probe and an NR-250 data collection system (Keyence, Osaka, Japan).

Net CO_2 assimilation rates were measured using an LI-7100 infrared CO_2/H_2O gas analyser (Li-Cor) attached to the gas-exchange chamber. At the beginning of the experiment, the leaf was exposed to a 9.17×10^{-3} dm^3 s^{-1} flow of 20% O_2 air containing 200 or 1000 ppm CO_2. After 30 min of stabilization of photosynthesis, CO_2 was switched to 99% $^{13}CO_2$ (Taiyo Nippon Sanso, Tokyo, Japan) at the same level (200 or 1000 ppm). After $^{13}CO_2$-feeding, a leaf disc (diameter 30 mm) was immediately freeze-clamped by liquid nitrogen in the gas-exchange chamber. The leaf disc was exposed to liquid nitrogen for 10 s and stored at –80 °C prior to the extraction of metabolites in the disc. Since the infrared absorption spectrum of $^{13}CO_2$ is different from that of $^{12}CO_2$, the infrared gas analyser is much less sensitive to $^{13}CO_2$ than to $^{12}CO_2$. The chlorophyll fluorescence of each sample leaf was measured before and after gas switching with a MINI-PAM photosynthesis yield analyser (Heinz Walz GmbH, Effeltrich, Germany) attached to the chamber.

Extraction of metabolites and measurement of ^{13}C-labelled fractions

The frozen leaf disc was homogenized by a Retsch ball-mill (Haan, Germany) at 20 Hz for 1 min. Hydrophilic tobacco metabolites were extracted using a solvent mixture of 500 μl of methanol and 20 μl of internal standard solution (100 μM of ribitol and PIPES)

by shaking at 37 °C for 5 min. After the addition of 500 µl of chloroform and 180 µl of water, the extracts were centrifuged at 10 000 *g* for 3 min. The supernatant was transferred to a new 1.5 ml tube, followed by the addition of 200 µl of water. After the mixture was centrifuged, the resultant polar phase was centrifugally filtered through an Ultrafree MC 5 kDa cutoff filter (Millipore, Billerica, MA, USA) at 10 000 *g* for 60 min. The filtrate was dried in a vacuum centrifugal concentrator. The residue was dissolved in 50 µl of water and analysed by CE-MS/MS.

All CE-MS/MS analyses were performed using a P/ACE MDQ (Beckman Coulter, Fullerton, CA, USA) and 4000QTRAP hybrid triple quadrupole linear ion-trap mass spectrometer with Turbo V ion source and CE-MS kit (Applied Biosystems, Foster City, CA, USA). An MP-711 micro flow pump (GL Sciences, Tokyo, Japan) was used to deliver the sheath liquid. Syringe pump Model 11 plus (Harvard Apparatus, Holliston, MA, USA) was used for infusing standard solutions for optimization of MRM detection. 32 Karat software (Beckman Coulter) controlled CE performance. MS/MS data acquisition, and data evaluation were controlled by Analyst software 1.4.1 (Applied Biosystems).

CE separations were carried out on a FunCap-CE type S capillary (GL Sciences). The capillary dimensions were 50 µm i.d. and 80 cm in length. The electrolyte for the CE separation was 50 mM ammonium acetate adjusted to pH 9.0 by the addition of ammonium hydroxide. Prior to the first use, each new capillary was washed with running electrolyte for 60 min with the application of 30 psi pressure. Before injection in each analysis, the capillary was pretreated with running electrolyte for 5 min by applying a pressure of 30 psi. The sample was injected at a pressure of 2.0 psi for 5.0 s (6 nl). The CE polarity was such that the electrolyte vial (inlet) was at the anode, and the ESI probe (outlet) was at the cathode. The applied voltage to the CE capillary was set at 30 kV with 0.30 min of ramp time. Electrophoresis was performed for 0–12 min. After stopping the application of voltage to CE at 12 min, the electrolyte was delivered through the capillary at 4.5 psi with an air pump for between 12 min and 16 min. The capillary temperature was maintained at 20 °C. The sheath fluid, 5 mM ammonium formate in 50% (v/v) acetonitrile/water was delivered to the electrospray probe at a rate of 10 µl min^{-1}. ESI-MS/MS was conducted in the negative ion mode. Ion spray voltage was applied at –4.5 kV only after 1 min of voltage application to the CE had passed. The setting for CE parameters were: curtain gas, 15.0 psi, collision gas, 5.0, temperature, 0.0, ion source gas 1, 20.0 psi, ion source gas 2, 0.0 psi, entrance potential, –10.0 V. Q1 and Q3 resolution were set as unit and low, respectively. CE-ESI-MS/MS analyses were performed as described previously (Harada *et al.*, 2008) except for the following conditions. All isotopomers of the analytes were quantified by MRM. Three types of runs of CE-ESI-MS/MS were performed per sample as shown in Table 1. The MRM parameters, Q1 (*m/z* of

Table 1. Method settings for isotopomer monitoring

Three types of runs of CE-MS/MS were performed per sample. The optimized parameters, Q1 (*m/z* of deprotonated precursor ion), Q3 (*m/z* of product ion), DP (declustering potential), CLE (collision energy), and collision cell exit potential (CXP) are listed. Dwell time of each MRM transition was set at 50 ms. PIPES, 1,4-piperazinediethanesulphonic acid.

Period	Analyte	Q1 (*m/z*)	Q3 (*m/z*)	DP (V)	CLE (V)	CXP (V)
Run 1						
1	None					
2	HP[1a]	259.0, 260.0, 261.0, 262.0, 263.0, 264.0, 265.0	97.0	–50	–22	–5
	PP[2b]	228.9, 229.9, 230.9, 231.9, 232.9. 233.9	97.1	–55	–18	–5
	Ribitol	151.0	89.0	–55	–16	–3
	PIPES	301.0	193.1	–85	–38	–13
	Total number of MRM: 15			Scan time: 0.825 s		
3	RuBP	308.9, 309.9, 310.9, 311.9, 312.9, 313.9	97.1	–45	–26	–5
	PGA	184.9, 185.9, 188.9, 187.9	97.0	–40	–20	–5
	PEP	166.9, 167.9, 168.9, 169.9	79.1	–40	–18	–1
	Total number of MRM: 14			Scan time: 0.770 s		
Run 2						
1	None					
2	Ribitol	151.0	89.0	–55	–16	–3
	Total number of MRM: 1			Scan time: 0.060 s		
3	S7P	289.0, 290.0, 291.0, 292.0, 293.0, 294.0, 295.0, 296.0	97.0	–55	–30	–5
	TP[a]	168.9, 169.9, 170.9, 171.9	97.0	–40	–14	–5
	PIPES	301.0	193.1	–85	–38	–13
	Total number of MRM: 16			Scan time: 0.880 seconds		
4	SBP	368.9, 369.9, 370.9, 371.9, 372.9, 373.9, 374.9, 375.9	97.1	–45	–30	–5
	FBP	339.0, 340.0, 341.0, 342.0, 343.0, 344.0, 345.0	97.1	–40	–30	–5
	Total number of MRM: 15			Scan time: 0.825 s		
Run 3						
1	None					
2	Ribitol	151.0	89.0	–55	–16	–3
	ADP-Glc	588.1, 589.1, 590.1, 591.1, 592.1, 593.1, 594.1	346.1	–95	–34	–3
	UDP-Glc	565.1, 566.1, 567.1, 568.1, 569.1, 570.1, 571.1	323.1	–85	–34	–1
	PIPES	301.0	193.1	–85	–38	–13
	Total number of MRM: 16			Scan time: 0.880 s		

[a] Hexose monophosphate (G6P, F6P, G1P).
[b] Pentose monophosphate (R5P, Ru5P/Xu5P).
[c] Triose monophosphate (GAP, DHAP).

deprotonated precursor ion), Q3 (*m/z* of product ion), declustering potential (DP), collision energy (CLE), and collision cell exit potential (CXP) are listed in Table 1. The DP, CLE, and CXP of all isotopomers were set to the same values.

Calculation of metabolic turnover

Relative isotopomer abundance (m_i) for each metabolite in which $i^{13}C$ atoms are incorporated is calculated by the following:

$$m_i(\%) = \frac{M_i}{\sum_{j=0}^{n} M_j} \times 100$$

where M_i represents the isotopomer abundance for each metabolite in which $i^{13}C$ atoms are incorporated.

The ^{13}C fraction of the metabolite possessing n carbon atoms is calculated by the following:

$$^{13}C\ \text{fraction}\ (\%) = \sum_{i=1}^{n} \frac{i \times m_i}{n}$$

Metabolic turnover rate was calculated from the initial slope of the ^{13}C-fration versus time curve, i.e. the change in the ^{13}C-fraction with respect to time from 0.5 min to 2 min because the highest value of correlation coefficient was shown at the time interval. In order to discuss the distribution of assimilated ^{13}C, the carbon turnover rate was estimated by dividing the initial slope by carbon number.

Results

Construction of ^{13}C-enrichment system

To analyse carbon metabolic turnover in fresh leaves, a system was developed for *in vivo* ^{13}C-labelling from $^{13}CO_2$ as shown in Fig. 2. The photosynthesis rate of an individual leaf was monitored in real time with a gas-exchange technique with light intensity, CO_2 concentration, relative humidity, and chamber temperature controlled. At the beginning of the experiment, the leaf carried out photosynthesis with unlabelled CO_2. After 30 min of stabilization of photosynthesis, ^{13}C-labelling was initiated by switching the CO_2 to $^{13}CO_2$ (Fig. 2B).

In photosynthesis, sugar phosphates turn over extremely fast. Theoretical calculations suggest that ribulose-1,5-*bis*phosphate (RuBP) pool turnover times of 0.5 s may occur [pool turnover rate (s)=pool size (μmol m^{-2})/assimilation rate (μmol m^{-2} s^{-1})] (Sharkey *et al.*, 1986). Therefore, it is important to quench metabolic reactions punctually and quickly for accurate kinetic analysis. In our system, a liquid nitrogen reservoir was mounted on the photosynthesis chamber. Photosynthetic reactions were quenched by flowing liquid nitrogen into the chamber. The labelled segment of the leaf was simultaneously cut in the chamber. A cutter was inserted from an access plate lying on the undersurface of the chamber (Fig. 2A). A PAM photosynthesis yield analyser was also attached to the chamber. The quantum yield of photosystem II (ΦPSII) of the tobacco leaf was not changed by switching gas from unlabelled CO_2 to $^{13}CO_2$ (data not shown), supporting the assumption that photosynthetic rate remains constant before and after labelling.

Determination of mass distribution of metabolites by CE-MS/MS

Sugar phosphates were separated by CE, and detected by MS/MS in MRM mode. The MRM method was optimized for the determination of each compound (Table 1) for the most sensitive detection because the amount of some sugar phosphates in plant cells is extremely small. Figure 3 shows the incorporation of ^{13}C in RuBP in tobacco leaves at various time points after the initiation of ^{13}C-labelling. The major precursor ion of RuBP was shifted from an unlabelled form (*m/z* 309) to the fully labelled form (*m/z* 314) within 10 min. Figure 4 shows the time-course of relative isotopomer abundance of each metabolite. Labelling started immediately after switching the gas to $^{13}CO_2$. The mass distribution of all metabolites determined was shifted to higher *m/z* with time. The most abundant isotopomer of phosphoglycerate (PGA), dihydroxyacetone-phosphate (DHAP), ribulose-5-phosphate (Ru5P), and sedoheptulose-7-phosphate (S7P), respectively, was shifted with time from m_0 (unlabelled form) to the fully labelled form in order of increasing incorporated ^{13}C number. Although the position of the labelled carbon could not be demonstrated by MS, ^{13}C seemed to be incorporated in turn. Our analytical system enabled kinetic determination of mass isotopomer distribution during photosynthetic dark

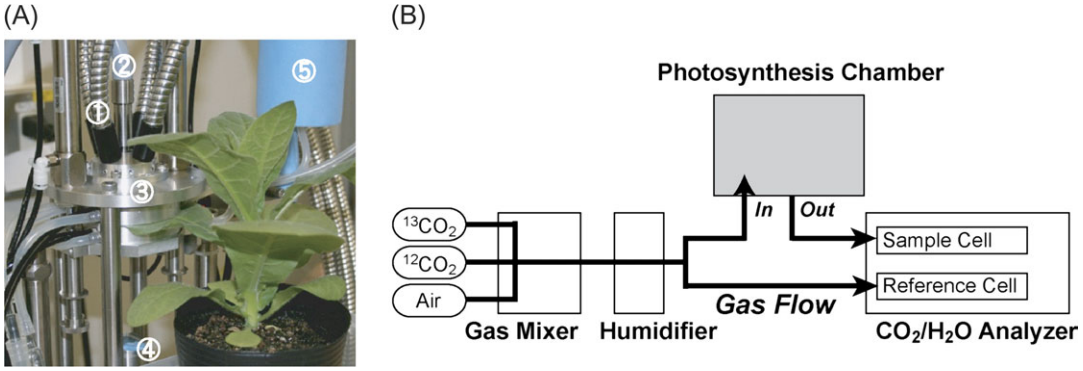

Fig. 2. Photosynthesis chamber for feeding $^{13}CO_2$ into a tobacco leaf (A) and flow path of mixed gasses (B). Air is 20% O_2 and 80% N_2. 1, light guide; 2, PAM probe; 3, gas-exchange chamber; 4, leaf cutter; 5, liquid nitrogen reservoir.

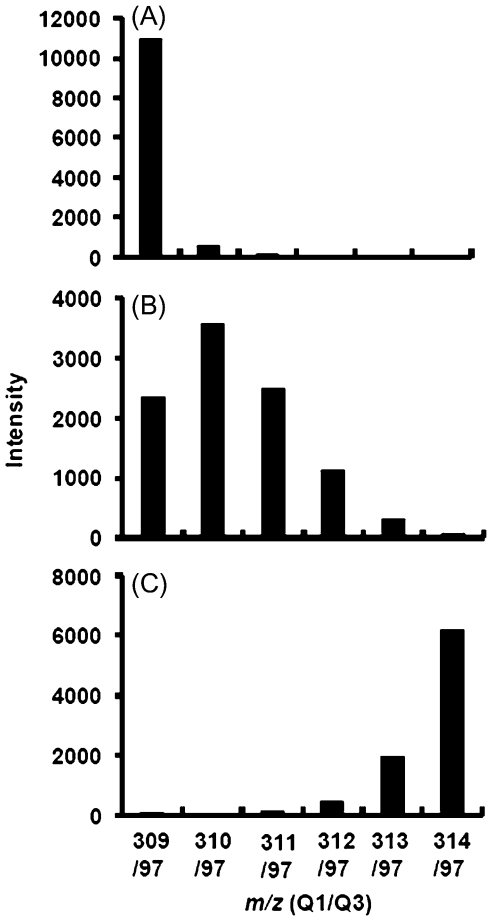

Fig. 3. Mass distribution of RuBP at 0 min (A), 1 min (B), and 10 min (C) after initiation of ^{13}C-labelling from $^{13}CO_2$. Q1, *m/z* of deprotonated precursor ion; Q3, *m/z* of product ion.

reactions occurring in a short time. The variability in three independent experiments was narrow.

Metabolic turnover analysis of sugar phosphates in fresh tobacco leaves

The ratio of ^{13}C to total carbon in each metabolite, i.e. the ^{13}C-fraction (%) was calculated from mass isotopomer distributions (Fig. 5). The ^{13}C-fraction of sugar phosphates increased with time and reached a plateau at a maximum value within 5–10 min under 1000 ppm CO_2. The time-course for the fraction of C as ^{13}C, i.e. the turnover rate of metabolites was determined under CO_2 concentrations of 1000 ppm and 200 ppm, which demonstrated an increase in the ^{13}C-fraction with an increase in CO_2 concentration. The photosynthetic rates of tobacco leaves were 18.3±2.5 and 4.5±1.3 μmol m^{-2} s^{-1} under 1000 and 200 ppm CO_2, respectively. The maximum value of the ^{13}C-fraction also showed a positive correlation with CO_2 concentration during photosynthesis. Under the 200 ppm CO_2 conditions, it took a longer time to reach the maximum value compared with the 1000 ppm conditions. The turnover rate of sugar phosphates involved in the Calvin cycle was significantly higher than that of organic acids and amino acids (Fig. 5; see Supplementary Fig. S1 at *JXB* online).

The maximum values of the ^{13}C-fraction in sugar phosphates involved in the Calvin cycle in tobacco leaves photosynthesizing in 1000 ppm CO_2 were between 83% and 93% (Fig. 5), which resulted from the last carbon atom not being completely labelled, as shown in Fig. 4. Even when extending the labelling time to 36 h under photosynthetic conditions, the ^{13}C-labelling ratio of metabolites did not reach 100%.

We tested whether metabolic flux from CO_2 might change throughout the diurnal cycle. For example, if the sugars and sugar phosphates produced by the degradation of starch during the night flow into the Calvin cycle after dawn (Weise *et al.*, 2006), carbon flux from CO_2 to sugar nucleotides such as ADP-glucose and UDP-glucose might change due to the flow from carbon derived from starch. However, in the present study, the ^{13}C-labelling rate of sugar phosphates did not differ in any photoperiod (data not shown).

The initial slope of the ^{13}C-fraction versus time curve (Fig. 5) is an estimate of the turnover rate of metabolites *in vivo*. Among sugar phosphates, G1P showed the lowest turnover rates (Fig. 6). Both G6P and G1P showed slower turnover rates than the other sugar phosphates. The carbon turnover rate of UDP-glucose was lower than that of ADP-glucose, which was comparable to that of G1P. The rate of ^{13}C-labelling depends on the pool size of each metabolite in the cells. As shown in Table 2, the level of G1P in tobacco leaves was 12 times less than that of G6P. These results suggest that the conversion of G6P into G1P is a rate-limiting step in the photosynthetic sugar biosynthesis pathway (Fig. 1).

Discussion

A novel system was developed for the determination of turnover rate during C_3 photosynthetic metabolism in the leaves of higher plants by the combination of an *in vivo* ^{13}C-labelling technique with $^{13}CO_2$ and mass isotopomer analysis using a CE-MS/MS profiling method. As shown in Fig. 4, the system enabled monitoring of the *de novo* synthesis of photosynthetic carbon metabolites at the carbon atom level and quantitative assessment of the turnover rate (Fig. 6).

The ^{13}C-labelling ratio of sugar phosphates was significantly higher than that of amino acids and organic acids. As for sugar phosphates involved in the Calvin cycle, a large fraction of carbons were labelled within 5 min after the initiation of ^{13}C-labelling under 1000 ppm CO_2 conditions. However, the ^{13}C-labelling ratio of G1P was only 41% at 5 min, which was a distinctly lower percentage than that of other sugar phosphates. The labelling ratio of G6P was 76% at the same time point. The pool size of G1P was one-twelfth that of G6P. The turnover rate of G1P was 38% of G6P under 1000 ppm CO_2 conditions (Fig. 6). Also, comparing the decay of m_0 for G1P and G6P showed a slower decay for G1P than G6P (Fig. 4). These results

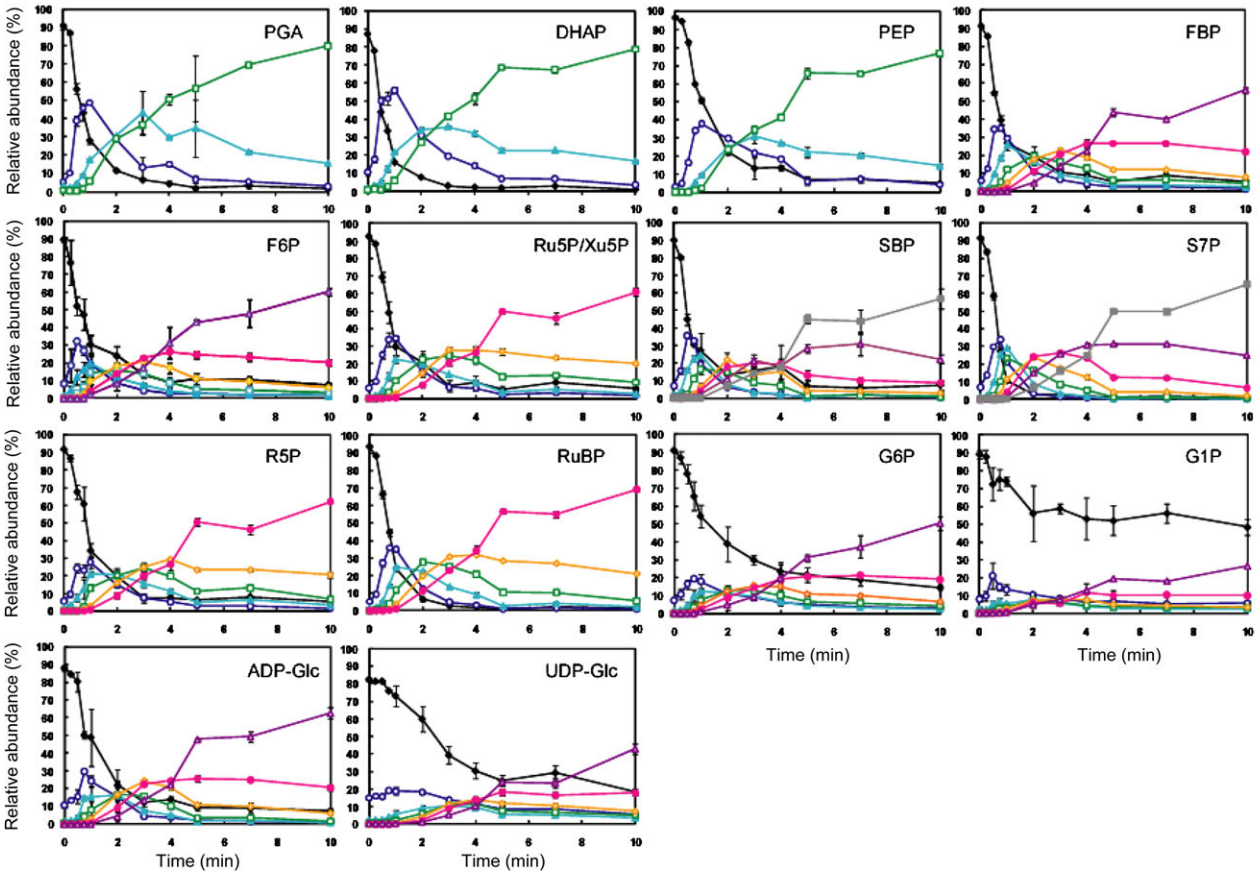

Fig. 4. Time-course of mass distribution of sugar phosphates in tobacco leaves under 1000 ppm $^{13}CO_2$ conditions. The mass distribution of ADP-glucose and UDP-glucose was calculated for the glucose moieties. Ru5P was not separated from Xu5P by capillary electrophoresis. Values are the averages of measurements of three different tobacco plants, ±SEM. Closed diamonds (black), m_0; open circles (blue), m_1; closed triangles (light blue), m_2; open squares (green), m_3; open diamonds (orange), m_4; closed circles (pink), m_5; open triangles (purple), m_6; closed squares (grey), m_7. m_i represents the relative isotopomer abundance for each metabolites in which $i^{13}C$ atoms are incorporated. 100% means the isotopomer abundance corresponds to the pool size of the metabolite.

indicate that conversion from G6P to G1P is a rate-limiting step of the sugar phosphate pathway.

The conversion of G6P to G1P is catalysed by phosphoglucomutase (PGM) in plant cells (Fig. 1). There are two PGM isoforms in plants, one localized in the plastids and the other in the cytosol (Periappuram *et al.*, 2000), that are considered to play a role in the allocation of carbon between sucrose and starch in leaves based on the analysis of a *Nicotiana sylvestris* mutant and a transgenic potato deficient in plastidial PGM (Huber and Hanson, 1992; Lytovchenko *et al.*, 2002*b*). However, the role of PGM in the control of carbon metabolic flux is not clear. PGM isoforms are present in high abundance in plant cells, and the reactions they catalyse are thought to operate close to equilibrium. Earlier ideas presented on metabolic regulation stated that near-equilibrium reactions could not exert much influence on the control of pathway flux (Rolleston, 1972). However, several recent reports have shown that other near-equilibrium reactions including plastidial aldolase (Haake *et al.*, 1998) and transketolase (Henkes *et al.*, 2001) can exert significant metabolic control *in vivo*. The expression of foreign PGM in the leaf cytosol or the repression of the activity of either cytosolic or plastidial PGM in potato leaves through genetic engineering led to alteration in the level of end-products such as starch and sucrose (Lytovchenko *et al.*, 2002*a*, *b*, 2005). However, the altered amount of the products was not proportional to the change in PGM activity in transgenic plants, lacking a sufficient explanation for rate control by the PGM reaction. Our results support that PGM controls the metabolic flux of sugar biosynthetic pathway based on direct measurement of the turnover rate of both substrate (G6P) and product (G1P), although it is difficult to discriminate among subcellular localization. As shown in Fig. 6, the metabolic turnover rate of UDP-glucose was lower than that of ADP-glucose (Fig. 6). PGM localized in the cytosol may contribute more to the control of metabolic flux than plastidial PGM.

In our analytical system, the variability in ^{13}C fraction (%) of metabolites is lower compared with the data in a previous report (Huege *et al.*, 2007) (Fig. 5). Since mass isotopomer distribution would be unaffected by matrix

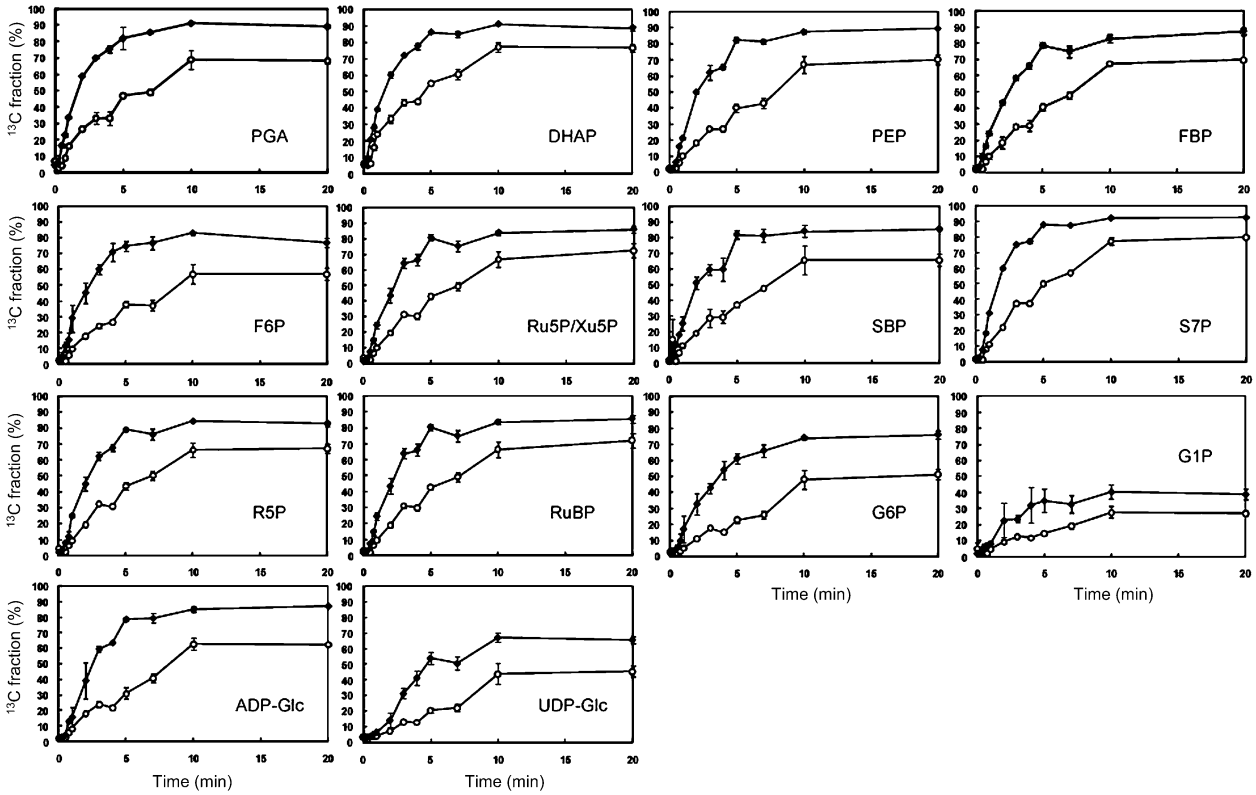

Fig. 5. Time-course for fraction of C as ^{13}C fraction in tobacco leaves under 200 ppm (circles) and 1000 ppm (filled diamonds) $^{13}CO_2$ conditions.

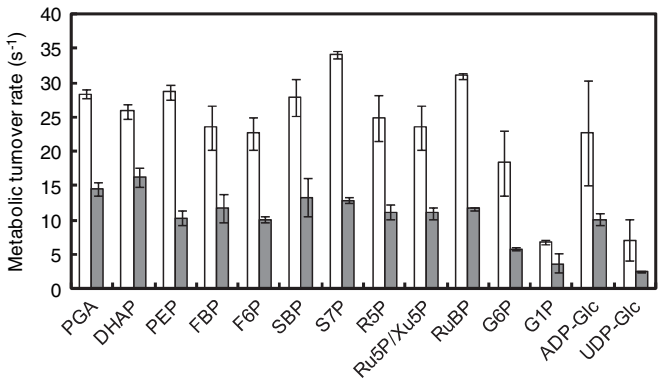

Fig. 6. Metabolic turnover rate of metabolites in tobacco leaves under 200 ppm (grey bars) and 1000 ppm (white bars) $^{13}CO_2$ condition. Values are the averages of measurements of three different tobacco plants, ±SEM.

effects that inhibit analyte ionization in the ion source of the mass spectrometer, the turnover rate would be precisely determined. In Table 2, some metabolites showed variation in the concentration. Since the amount of some sugar phosphates and sugar nucleotides is extremely small, the resolution of the MS data that is sometimes acquired around the detection limits is not necessarily high (Cruz *et al.*, 2008). However, in the present study, the metabolic turnover and carbon distribution during photosynthetic dark reactions occurring in a short time are discussed.

Although it is possible to observe rapid metabolic turnover in cells by using our analytical system, it is impossible to distinguish subcellular localization of metabolite pools. Practically, after quenching of metabolic reactions by liquid nitrogen, fractionation of organelle cannot be accomplished. Thus, the localization of rate-limiting steps could not be demonstrated. However, a possible distinction between compartments could be indicated. As shown in Fig. 4, while the decay of m_0 for the RuBP that exists only in plastids is fast, the decay of m_0 for other metabolites such as FBP, F6P, and R5P that exist in both plastids and cytosol shows at least a two-phase alteration. Multi-phase alteration of m_0 decay might result from the cellular compartmentation of metabolic reactions. Also, the m_0 decay of UDP-glucose changes from a low rate, like the m_0 decay of G1P, to a high rate, like that of G6P, 2 min after the start of ^{13}C-labelling. The turnover of UDP-glucose might be related to the rate of conversion from G6P to G1P in the cytosol.

An increase in CO_2 concentration from 200 ppm to 1000 ppm led to a rise in the turnover rate of intermediate compounds (Fig. 6) as well as the photosynthesis rate, indicating that the increase in the ambient CO_2 led to the acceleration of carbon metabolic flux. The alterations in the turnover rate were different among compounds. For example, phosphoenolpyruvate (PEP) and G6P, respectively, showed 2.8- and 3.1-fold increases in carbon turnover on changing CO_2 concentration from 200 ppm to 1000 ppm, whereas DHAP, PGA, and G1P, respectively,

showed only 1.9-, 1.6-, and 1.8-fold increases. Therefore, the responsiveness of turnover to CO_2 concentration is different among the metabolic reactions. The turnover rate of G1P showed lower responsiveness to CO_2 concentration than that of G6P, which also supports the hypothesis of PGM being a rate-limiting step of photosynthetic sugar biosynthesis pathway.

Surprisingly, the turnover of PEP was as fast as that of sugar phosphates (Fig. 6). Phosphoenolpyruvate dehydratase (enolase) catalyses the conversion of PGA to PEP during glycolysis; its plastid isoform has not been found in *Arabidopsis thaliana* (Van der Straeten *et al.*, 1991). PEP is a precursor of pyruvate, which is used for the biosynthesis of amino acids and organic acids via the tricarboxylic acid (TCA) cycle, and of fatty acids from acetyl-CoA. Also, PEP is a substrate of PEP carboxylase and PEP carboxykinase to produce oxaloacetate, which is concerned with CO_2 assimilation in C_4 photosynthesis. Therefore, it is of interest to analyse the turnover of metabolites that are downstream of PEP as a next step for research.

In order to discuss the distribution of assimilated ^{13}C, carbon turnover rate was estimated by dividing the metabolic turnover rate by the number of carbons that constitute each metabolite. As shown in Fig. 6, the response of the carbon turnover rate to CO_2 assimilation rate is different among metabolites. The difference should be explained by the ^{13}C distribution. Although it is not certain that all carbons of metabolites are equally replaced into ^{13}C by turnover, the estimation of carbon turnover rate would enable us to consider the flux of carbon distribution. Thus, the ratio of the carbon turnover rate to the CO_2 assimilation rate (*T*/*A* ratio) under different CO_2 conditions was shown in Table 3. To estimate the *T*/*A* ratio, net photosynthesis rate was used because the rate of CO_2 evolution would be negligible under the condition of high light intensity (1000 μmol photons m^{-2} s^{-1}) as described in a previous paper (Brooks and Farquhar, 1985). The T/A ratio is lower under 1000 ppm CO_2 than 200 ppm CO_2 conditions. The data indicate that the efficiency of the use of carbon from CO_2 for metabolism became lower at higher CO_2 concentration. On the basis of Farquhar's photosynthesis models (Farquhar *et al.*, 1980, 2001; Sharkey, 1985), the assimilation rate of CO_2 in leaves is limited by Rubisco activity under low CO_2, and is limited by RuBP regeneration, which is dependent on the energy (ATP and NADPH) supplied by electron transport in photosystem complexes at above ambient (380 ppm) CO_2 concentration. Therefore, the decrease in the carbon use efficiency under 1000 ppm CO_2 (Table 3) might be limited by the supply of the energy substrates.

As shown in Fig. 5, the ^{13}C-fraction of metabolites did not reach 100% under the 1000 ppm CO_2 conditions that maximized the CO_2 assimilation rate of tobacco leaves. Another report found that, in leaves of *Quercus rubra* exposed to 35 Pa $^{13}CO_2$ under 500 μmol m^{-2} s^{-1} light conditions, the ^{13}C-labelling ratio of PGA finally reached 84% after 18 min of ^{13}C-treatment (Delwiche and Sharkey, 1993). Although the cause of peaking below 100% is still unknown, one of the likely explanations is that newly assimilated carbon competes with carbon derived from internal stores and an equilibrium phase is reached after the initial linear enrichment phase. Although transitory starch degradation could be regulated by light, circadian rhythms, or carbon balance, under photorespiratory conditions, transitory starch breakdown occurs in the light and G6P is elevated (Weise *et al.*, 2006). G6P is the product of phosphorolytic breakdown of transitory starch, which may be used to regenerate

Table 2. Comparison of metabolite pools in tobacco leaves

The value for Ru5P/Xu5P represents the sum of Ru5P and Xu5P content. Values are averages from measurements of three different tobacco plants, ±SEM. Leaf discs were exposed to an air stream containing 1000 ppm CO_2 for 30 min in a gas exchange chamber before sampling.

Metabolite	Concentration (μmol m^{-2})
PGA	3.5±0.8
DHAP	10.5±6.6
PEP	1.0±0.2
FBP	0.6±0.0
F6P	16.8±1.1
SBP	0.1±0.0
S7P	70.3±3.3
R5P	4.5±4.3
Ru5P/Xu5P	14.1±8.1
RuBP	10.0±1.4
G6P	31.0±19.0
G1P	2.5±1.7
ADP-Glc	0.9±0.2
UDP-Glc	9.3±2.5

Table 3. Ratio of carbon turnover rate to CO_2 assimilation rate under different CO_2 conditions

Values are averages from measurements of three different tobacco plants, ±SEM.

Compound	*T*/*A* ratio (carbon turnover/CO_2 assimilation)		Rate of decrease in *T*/*A* ratio
	C_a=200 ppm (*A*=4.5±1.3 μmol m^{-2} s^{-1})	C_a=1000 ppm (*A*=18.3±2.5 μmol m^{-2} s^{-1})	
PGA	1.08±0.07	0.52±0.01	0.48
DHAP	1.20±0.11	0.47±0.02	0.39
PEP	0.76±0.07	0.52±0.02	0.68
FBP	0.43±0.07	0.21±0.03	0.50
F6P	0.37±0.02	0.21±0.02	0.55
SBP	0.42±0.09	0.22±0.02	0.51
S7P	0.41±0.01	0.27±0.00	0.65
R5P	0.50±0.05	0.27±0.04	0.55
Ru5P/Xu5P	0.49±0.04	0.26±0.03	0.52
RuBP	0.52±0.01	0.34±0.00	0.65
G6P	0.22±0.01	0.17±0.04	0.77
G1P	0.14±0.05	0.06±0.00	0.46
ADP-Glc	0.37±0.03	0.21±0.07	0.55
UDP-Glc	0.09±0.00	0.06±0.03	0.69

Calvin cycle intermediates. Sucrose cleavage is catalysed by invertase (sucrose+$H_2O \rightarrow$glucose+fructose) or sucrose synthase (sucrose+UDP$\leftarrow \rightarrow$fructose+UDP-glucose) (Baroja-Fernández *et al.*, 2001; Koch, 2004). Glucose and fructose could be phosphorylated to produce G6P and F6P, respectively by hexokinase. UDP-glucose could be a substrate of UDP-glucose pyrophosphorylase to produce UTP and G1P. However, it remains to be seen whether degradation products of storage saccharides flow in the opposite direction to carbon assimilation in leaves under photosynthetic conditions. Another possibility for the plateau in the ^{13}C-labelling ratio is intracellular compartmental flux. In plant cells, most metabolites are present in two or more pools, which exhibit slow exchange rates. One of these pools would be required to be metabolically inert, for example, the vacuole or possibly the apoplast. Although Winter *et al.* (1994) estimated the subcellular metabolite concentrations in spinach leaves based on the measurement of the volume of cellular and subcellular compartments, the concentration of sugar phosphate was much lower in the vacuole than in both the stroma and the cytosol. Another explanation for lower than 99% labelling is that not all cells are equally photosynthetically active. The leaf is a mixture of many different cell types since some may be old and senescent and act as storage cells. Certain cell types would not be metabolically active. However, in the present study, when extending the labelling time to 36 h, the ^{13}C-labelling ratio of metabolites still did not reach 100%.

So far, metabolic profiling techniques (Fiehn *et al.*, 2000; Roessner *et al.*, 2000; Sato *et al.*, 2004; Cruz *et al.*, 2008; Harada *et al.*, 2008) have enabled the analysis of a large number of metabolites, including minor intermediates, simultaneously by using MS, which has high sensitivity, high mass resolution, and high scan speed. However, the information available from this technique is a snapshot at the time of sampling the metabolites. To estimate dynamic metabolic flux, a combination with *in vivo* labelling by means of a stable isotope is required. Thus, a novel ^{13}C-enrichment system was developed with $^{13}CO_2$ to analyse the metabolic flux of the C_3 photosynthetic pathway. Detection of mass isotopomer abundance by CE-MS/MS enabled quantification of the metabolic turnover rate of minor intermediates such as sugar phosphate and sugar nucleotides in tobacco leaves for the first time. Our analytical system would also be useful for the elucidation of the mechanism of metabolic responses to stress and other alterations in ambient conditions such as temperature and CO_2 influx as well as for the identification of rate-limiting steps in metabolic pathways. In aiming to produce useful compounds in transgenic plants through metabolic engineering, the enhancement of the activity of a rate-limiting enzyme in a pathway could be an efficient means to increase the metabolic flux of target compounds. Plants assimilate CO_2 as a carbon source and produce a large number of substances. Starch, sucrose, and cellulose are major forms of biomass. Among secondary metabolites such as fatty acids, isoprenoids, and flavonoids, there are a number of compounds used as industrial products. This study's approach should provide a powerful tool for the evaluation of the carbon allocation and turnover of carbon metabolism in higher plants.

Supplementary data

Supplementary data are available at *JXB* online.

Supplementary Fig. S1. Time-course of ^{13}C fraction of amino acids and organic acids in tobacco leaves.

Acknowledgements

This work has been supported through project P02001 (directed by Professor A Shinmyo) by the New Energy and Industrial Technology Development Organization (NEDO), under the sponsorship of the Ministry of Economy, Trade, and Industry (METI) of Japan. The authors are grateful to Yohko Ohyama (Osaka University, Japan) for her technical support, and offer heartfelt condolences to her.

References

Baroja-Fernández E, Muñoz FJ, Akazawa T, Pozueta-Romero J. 2001. Reappraisal of the currently prevailing model of starch biosynthesis in photosynthetic tissues: a proposal involving the cytosolic production of ADP-glucose by sucrose synthase and occurrence of cyclic turnover of starch in the chloroplast. *Plant and Cell Physiology* **42,** 1311–1320.

Brooks A, Farquhar GD. 1985. Effect of temperature on the CO_2/O_2 specificity of ribulose-1,5-*bis*phosphate carboxylase/oxygenase and the rate of respiration in the light. *Planta* **165,** 397–406.

Cruz JA, Emery C, Wüst M, Kramer DM, Lange BM. 2008. Metabolic profiling of Calvin cycle intermediates by HPLC-MS using mixed-mode stationary phases. *The Plant Journal* **55,** 1047–1060.

Delwiche CF, Sharkey TD. 1993. Rapid appearance of ^{13}C in biogenic isoprene when $^{13}CO_2$ is fed to intact leaves. *Plant, Cell and Environment* **16,** 587–591.

Dennis DT, Blakeley SD. 2000. Carbohydrate metabolism. In: Buchanan W, Gruissem R, Jones R, eds. *The biochemistry and molecular biology of plants*. Rockville, MD: American Society of Plant Physiologists, 630–675.

Farquhar GD, von Caemmerer S, Berry JA. 1980. A biochemical model of photosynthetic CO_2 assimilation in leaves of C_3 species. *Planta* **149,** 78–90.

Farquhar GD, von Caemmerer S, Berry JA. 2001. Models of photosynthesis. *Plant Physiology* **125,** 42–45.

Fiehn O, Kopka J, Dörmann P, Altmann T, Trethewey RN, Willmitzer L. 2000. Metabolite profiling for plant functional genomics. *Nature Biotechnology* **18,** 1157–1161.

Giersch C. 2000. Mathematical modelling of metabolism. *Current Opinion in Plant Biology* **3,** 249–253.

Haake V, Zrenner R, Sonnewald U, Stitt M. 1998. A moderate decrease of plastid aldolase activity inhibits photosynthesis, alters the

levels of sugars and starch, and inhibits growth of potato plants. *The Plant Journal* **14,** 147–157.

Harada K, Ohyama Y, Tabushi T, Kobayashi A, Fukusaki E. 2008. Quantitative analysis of anionic metabolites for *Catharanthus roseus* by capillary electrophoresis using sulfonated capillary coupled with electrospray ionization-tandem mass spectrometry. *Journal of Bioscience and Bioengineering* **105,** 249–260.

Harrison EP, Willingham NM, Lloyd JC, Raines CA. 1998. Reduced sedoheptulose-1,7-*bis*phosphatase levels in transgenic tobacco lead to decreased photosynthetic capacity and altered carbohydrate accumulation. *Planta* **204,** 27–36.

Harrison EP, Olçer H, Lloyd JC, Long SP, Raines CA. 2001. Small decreases in SBPase cause a linear decline in the apparent RuBP regeneration rate, but do not affect Rubisco carboxylation capacity. *Journal of Experimental Botany* **52,** 1779–1784.

Henkes S, Sonnewald U, Badur R, Flachmann R, Stitt M. 2001. A small decrease of plastidial transketolase activity in antisense tobacco transformants has dramatic effects on photosynthesis and polypropanoid metabolism. *The Plant Cell* **13,** 535–551.

Huber SC, Hanson KR. 1992. Carbon partitioning and growth of a starchless mutant of *Nicotiana sylvestris*. *Plant Physiology* **99,** 1449–1454.

Huege J, Sulpice R, Gibon Y, Lisec J, Koehl K, Kopka J. 2007. GC-EI-TOF-MS analysis of *in vivo* carton-partitioning into soluble metabolite pools of higher plants by monitoring isotope dilustion after $^{13}CO_2$ labelling. *Phytochemistry* **68,** 2258–2272.

Koch K. 2004. Sucrose metabolism: regulatory mechanisms and pivotal roles in sugar sensing and plant development. *Current Opinion in Plant Biology* **7,** 235–246.

Koßmann J, Sonnewald U, Willmitzer L. 1994. Reduction of the chloroplastic fructose-1,6-*bis*phosphatase in transgenic potato plants impairs photosynthesis and plant growth. *The Plant Journal* **6,** 637–650.

Kruckeberg AL, Neuhaus HE, Feil R, Gottlieb LD, Stitt M. 1989. Decreased-activity mutants of phosphoglucose isomerase in the cytosol and chloroplast of *Clarkia xantiana*. *Biochemical Journal* **261,** 457–467.

Lytovchenko A, Sweetlove L, Pauly M, Fernie AR. 2002*a*. The influence of cytosolic phosphoglucomutase on photosynthetic carbohydrate metabolism. *Planta* **215,** 1013–1021.

Lytovchenko A, Bieberich K, Willmitzer L, Fernie AR. 2002*b*. Carbon assimilation and metabolism in potato leaves deficient in plastidial phosphoglucomutase. *Planta* **215,** 802–811.

Lytovchenko A, Hajirezaei M, Eickmeier I, Mittendorf V, Sonnewald U, Willmitzer L, Fernie AR. 2005. Expression of an *Escherichia coli* phosphoglucomutase in potato (*Solanum tuberosum* L.) results in minor changes in tuber metabolism and a considerable delay in tuber sprouting. *Planta* **221,** 915–927.

Ölçer H, Lloyd JC, Raines CA. 2001. Photosynthetic capacity is differentially affected by reductions in sedoheptulose-1,7-*bis*phosphatase activity during leaf development in transgenic tobacco plants. *Plant Physiology* **125,** 982–989.

Paul MJ, Knight JS, Habash D, Parry MAJ, Lawlor DW, Barnes SA, Loynes A, Gray JC. 1995. Reduction in phosphoribulokinase activity by antisense RNA in transgenic tobacco: effect on CO_2 assimilation and growth in low irradiance. *The Plant Journal* **7,** 535–542.

Periappuram C, Steinhauer L, Barton DL, Taylor DC, Chatson B, Zou J. 2000. The plastidic phosphoglucomutase from Arabidopsis. A reversible enzyme reaction with an important role in metabolic control. *Plant Physiology* **122,** 1193–1200.

Poolman MG, Fell DA, Thomas S. 2000. Modelling photosynthesis and its control. *Journal of Experimental Botany* **51,** 319–328.

Price GD, Evans JR, von Caemmerer S, Yu J-W, Badger MR. 1995. Specific reduction of chloroplast glyceraldehyde-3-phosphate dehydrogenase activity by antisense RNA reduces CO_2 assimilation via a reduction in ribulose bisphosphate regeneration in transgenic tobacco plants. *Planta* **195,** 369–378.

Roessner U, Wagner C, Kopka J, Trethewey RN, Willmitzer L. 2000. Simultaneous analysis of metabolites in potato tuber by gas chromatography-mass spectrometry. *The Plant Journal* **23,** 131–142.

Rolleston FS. 1972. A theoretical background to the use of measured intermediates in the study of the control of intermediary metabolism. *Current Topics in Cellular Regulation* **5,** 47–75.

Sato S, Soga T, Nishioka T, Tomita M. 2004. Simultaneous determination of the metabolites in rice leaves using capillary electrophoresis mass spectrometry and capillary electrophoresis diode array detection system. *The Plant Journal* **40,** 151–163.

Schwender J. 2008. Metabolic flux analysis as a tool in metabolic engineering of plants. *Current Opinion in Biotechnology* **19,** 131–137.

Sharkey TD. 1985. Photosynthesis in intact leaves of C_3 plants: physics, physiology and rate limitations. *The Botanical Review* **51,** 53–105.

Sharkey TD, Seeman JR, Berry JA. 1986. Regulation of ribulose-1,5-bisphosphate carboxylase activity in response to changing partial pressure of O_2 and light in *Phaseolus vulgaris*. *Plant Physiology* **81,** 788–791.

Tamoi M, Nagaoka M, Yabuta Y, Shigeoka S. 2005. Carbon metabolism in the Calvin cycle. *Plant Biotechnology* **22,** 355–360.

van der Straeten D, Rodrigues-Pousada RA, Goodman HM, Van Montagu M. 1991. Plant enolase: gene structure, expression, and evolution. *The Plant Cell* **3,** 719–735.

Weise SE, Schrader SM, Kleinbeck KR, Sharkey TD. 2006. Carbon balance and circadian regulation of hydrolytic and phosphorolytic breakdown of transitory starch. *Plant Physiology* **141,** 879–886.

Winter H, Robinson DG, Heldt HW. 1994. Subcellular volumes and metabolite concentrations in spinach leaves. *Planta* **193,** 530–535.

Zeeman SC, Smith SM, Smith AM. 2007. The diurnal metabolism of leaf starch. *Biochemical Journal* **401,** 13–28.

Zhu X-G, de Sturler E, Long SP. 2007. Optimizing the distribution of resources between enzymes of carbon metabolism can dramatically increase photosynthetic rate: a numerical simulation using an evolutionary algorithm. *Plant Physiology* **145,** 513–526.